

# Agglomeration equilibria of hematite nanoparticles



Kenichi Shimizu, Stanislav V. Sokolov, Richard G. Compton \*

Department of Chemistry, Physical and Theoretical Chemistry Laboratory, Oxford University, South Parks Road, Oxford, OX1 3QZ, United Kingdom

## ARTICLE INFO

### Article history:

Received 5 March 2016

Received in revised form 9 June 2016

Accepted 21 June 2016

Available online xxxx

### Keywords:

Hematite

Agglomeration

Nanoparticles

Chronoamperometry

pH

## ABSTRACT

Nanoparticle agglomeration is a naturally occurring physicochemical process which is utilized for environmental remediation. Investigations of agglomeration equilibria have hitherto been challenging because of the lack of an appropriate in-situ analytical method. We investigate dynamic equilibria between individual and agglomerated hematite nanoparticles in 20 mM KCl solution at pH between 2.0 and 4.0 using the newly established particle-impact chronoamperometry. The results reveal that the electrochemical technique primarily detects individual  $\text{Fe}_2\text{O}_3$  nanoparticles dissociated from the agglomerates indicative of the rapid and reversible nature of the agglomeration/dis-agglomeration process. A shift of the agglomeration equilibria towards cluster formation as pH increases from 2.0 to 4.0 is made apparent by the changes in the relative number and the size distribution of the monomeric nanoparticles detected. The work demonstrated herein opens a new way of investigating the agglomeration behavior of mineral nanoparticles in aquatic media.

© 2016 Elsevier B.V. This is an open access article under the CC BY-NC-ND license (<http://creativecommons.org/licenses/by-nc-nd/4.0/>).

## 1. Main text

Hematite ( $\alpha\text{-Fe}_2\text{O}_3$ ) is a naturally ubiquitous mineral and is the most thermodynamically stable form of iron oxide in the Earth's upper crust [1]. Owing to its photoelectrocatalytic properties, it has gained significant technological interest in recent years [2]. This mineral also plays various important roles in natural settings. In particular it is an effective adsorbent for various pollutants, such as natural organic matters [3] and (in)organic colloidal particles [4], that are then removed from the groundwater or transported. The ability of the colloidal iron oxide to remediate groundwater is becoming increasingly important due to the vast amounts of engineered nanomaterials that have been released into the natural water systems in recent years [5]. Sedimentation promoted by agglomeration with the naturally occurring nanoparticles is a key process to determine the fate of potentially toxic nanomaterials of anthropogenic origins in aquatic systems [6]. In this respect, knowledge of the dynamic equilibria of hematite nanoparticles agglomeration in an aqueous solution is essential.

The term "agglomeration" used throughout this article describes a reversible adhesion of dispersed particles driven by weak physical forces [7]. This is in contrast to aggregation, which IUPAC [7] defines as an irreversible assemblage of nanoparticles. For minerals, whose chemical properties are defined by their crystal structure, aggregate formation occurs under special circumstances such as at 100 °C for hematite during forced hydrolysis, whereas individual particles in agglomerates are

separated by grain boundaries. Agglomeration behavior of nanoparticles has been challenging to investigate using conventional methods. For instance, electron microscopies require drying samples before analysis, which itself induces the formation of agglomerates [8]. Nanoparticle tracking analysis (NTA) is more suitable for the purpose because of its ability to track individual diffusible entities [9]. Still, this technique is largely indiscriminate and requires careful analysis to determine the size of monomers; it is also limited to relatively large nanoparticles (>30 nm), nor it can be applied to optically opaque media. Particle-impact chronoamperometry offers a unique alternative way of particle sizing that can complement the conventional methods to investigate dynamics of hematite agglomeration. Based on the random motion of dispersed nanoparticles to collide with a stationary microelectrode, this electrochemical technique has been successfully utilized for the characterization of various nanoparticle systems [10–12]. This technique has been applied to address the reversible nature of silver nanoparticle agglomeration in aqueous solutions that contained various concentrations of KCl to provide proof-of-concept for this study [13]. Further investigation has shown that, when the agglomeration/dis-agglomeration process is sufficiently faster than the voltammetric time-scale (i.e.  $r^2/D$  where  $r$  is the radius of the microelectrode and  $D$  is the diffusion coefficient of a nanoparticle), this technique preferentially detects dis-agglomerated particles, or monomers, that are less affected by the near-wall diffusional hindrance than larger clusters [14]. This technique is therefore employed herein to obtain insights into the agglomeration behavior of the  $\text{Fe}_2\text{O}_3$  mineral in a simple aqueous solution of 20 mM KCl. The pH of the electrolyte solution was varied between 2.0 and 4.0 using 20 mM HCl prior to the addition of hematite. In light of

\* Corresponding author.

E-mail address: [Richard.Compton@chem.ox.ac.uk](mailto:Richard.Compton@chem.ox.ac.uk) (R.G. Compton).

the point of zero charge of the mineral being ca. 9.2 [15], the fundamental mechanism of nanoparticles agglomeration is expected to be the same as at pHs more commonly found in the natural environment; the pH of this study provides better colloidal stability. There was no significant change in the pH of the electrolyte solution after the addition of hematite nanoparticles. Under the experimental conditions, the ionic strength is below the critical coagulation concentration, which also ensures the stability of colloidal suspension [15], while it is high enough for the electrochemical reaction to be fully diffusion controlled [10].

Hematite nanoparticles studied in this work were prepared previously [16] by forced hydrolysis and stored in a suspension in the dark. Initial assessment of size distribution of monomers was carried out using transmission electron microscopic (TEM) images (Fig. 1). The mean diameter of 538 individual particles identified from the TEM images was  $35.3 \pm 4.5$  nm. The inset of Fig. 1 shows clustered nanoparticles, which probably formed during the deposition onto a copper grid. Individual particles have a quasi-spherical shape, as expected for synthetic hematite prepared by the hydrothermal method [15]. No chemical impurity was detected from the colloidal hematite by an X-ray photoelectron spectroscopic analysis (a Kratos Axis Ultra electron spectrometer, result not shown). Powder X-ray diffraction spectroscopy (a Bruker d8 Advance X-ray diffractometer) was used to ensure that this synthetic mineral has the rhombohedral structure, a characteristic crystal structure of hematite,  $\alpha\text{-Fe}_2\text{O}_3$  [17], (result not shown).

An independent assessment of particle agglomeration with respect to pH is provided by NTA, which was performed by placing a small aliquot of hematite pre-dispersed in either 20 mM KCl solution or in pure water in a thin optical cell. A NanoSight LM20 system (Malvern Instrument) equipped with a 640 nm laser source and a  $20\times$  magnification objective lens was used to visualize the particles. A video of the Brownian motion of the suspended hematite particles/clusters was recorded for the duration of 1 min. It was then processed using the NTA 3.1 analysis software to obtain a size distribution, which is summarized in the histogram (Fig. 2a). This measurement was repeated to ensure reproducibility of the observations. Hematite nanoparticles dispersed in ultrapure water (Fig. 2a, top histogram) shows the mean diameter of 65 nm and majority of signals are collected from the particles smaller than 110 nm. This relatively narrow size distribution is comparable to that from TEM images shown in Fig. 1. Agglomeration is observable from hematite nanoparticles dispersed in the pH 2.0 system (Fig. 2a, second from the top). This occurs partly because the addition of electrolyte ion decreases the dielectric constant of the aqueous solution and the electrostatic repulsion between nanoparticles, in accordance to the Derjaguin-Landau-Verwey-Overbeek (DLVO) theory [15] and partly to maximize the entropy of mixing of the system [18]. Nonetheless, the degree of agglomeration is low at this pH; the size distribution is rather similar to that in ultrapure water.

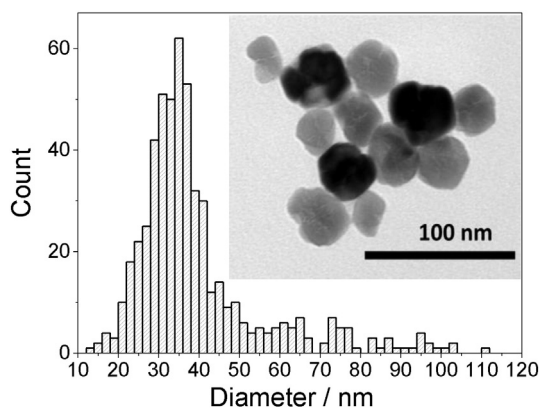


Fig. 1. Histogram showing the size distribution of hematite nanoparticles based on the measurements of 538 individual particles captured in TEM images. The mean diameter is found at  $35.3 \pm 4.5$  nm. Inset: a representative TEM image of hematite nanoparticles.

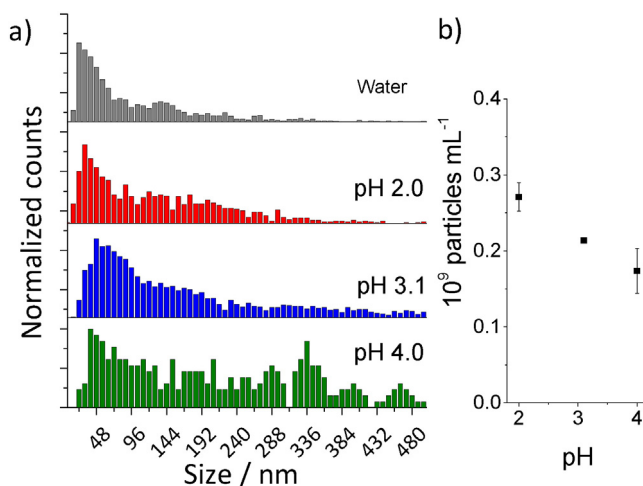
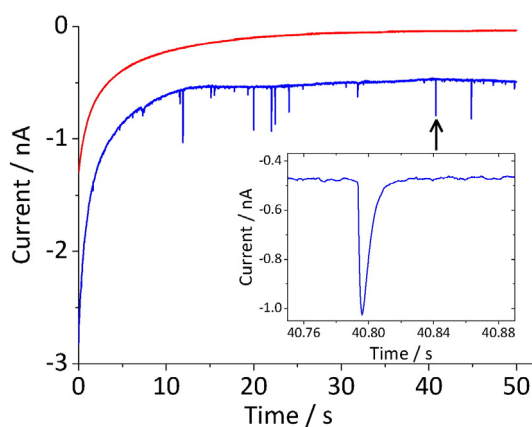


Fig. 2. a) Histograms of the size distribution of hematite based on NTA. The top histogram is from hematite nanoparticles dispersed in ultrapure water while in others it was dispersed in 20 mM KCl at pH as noted in the figure. b) The concentration of detectable entities in each pH system as measured from NTA. Standard error of the mean is shown in the figure.

At pH 3.1, the histogram shows that the size distribution has shifted towards larger particles (Fig. 2a, second from the bottom) indicating enhanced agglomeration above pH 2.0. This may be attributable to the surface potential of hematite particles being decreased by the increase in pH as predicted by the surface complexation model [19]. Metal oxides are particularly sensitive to solution pH as the surface consists of oxy(hydr)oxide functional groups [19]. The highest degree of cluster formation in this study is observed at pH 4.0 (Fig. 2a, bottom), as indicated by the widest size distribution and a significant decrease in the concentration of the detectable entities (Fig. 2b). Fewer signals are also seen in the NTA experiment of the agglomerated sample because the larger entities diffuse more slowly. Based on these results, it is evident that agglomeration occurs at pH between 2.0 and 4.0, as indicated by the widening of the size distribution. It cannot be confirmed from the histograms, however, whether there is an equilibrium between individual and agglomerated nanoparticles. For that, particle-impact chronoamperometry is particularly useful to monitor monomers as larger agglomerates are less detectable due to their slow diffusion.

Particle-impact chronoamperometry was conducted using a conventional three-electrode setup and a Metrohm  $\mu$ Autolab II potentiostat (Utrecht, the Netherlands) with Nova (v.1.11.2) as an operating interface. Prior to the experiment, the metal oxide nanoparticles ( $42 \text{ mg L}^{-1}$  or  $0.46 \text{ nM}$  estimated based on the particle size of  $35.3 \text{ nm}$  in diameter) were thoroughly dispersed in degassed 20 mM KCl at pH between 2.0 and 4.0 by ultrasonic agitation for 5 min. A minimum of thirty five chronoamperograms were recorded at each pH at  $25^\circ\text{C}$  at a well-polished gold microelectrode ( $11 \mu\text{m}$  in diameter) for the duration of 50 s at the applied potential between  $-0.4 \text{ V}$  and  $-0.2 \text{ V}$  vs. standard calomel electrode (SCE,  $0.242 \text{ V}$  vs. normal hydrogen electrode). Chronoamperograms recorded in the presence of hematite nanoparticles show reductive spikes (Fig. 3) indicative of the reduction of the iron oxide to ferrous ions upon collision with a stationary working electrode [20]. The shape of the spike depicted in the figure which is consistently observed throughout this study results from the electro-dissolution process being faster than the bandwidth of filter used in the potentiostat. Nevertheless, the original charge generated from the electrochemical process is fully conserved by the electronics of the system [21]. Sufficiently high potentials are applied to ensure that the reduction of hematite nanoparticles is diffusion controlled (the most cathodic overpotential for this process at pH 2 is reportedly at around  $+0.25 \text{ V}$  vs SCE [20]). This is also confirmed in this study



**Fig. 3.** Representative current-time profiles of particle-impact chronoamperometry collected in 20 mM KCl at pH 3.1 at  $-0.3$  V vs. SCE in the presence (blue line) and absence (red line) of ca. 0.46 nM hematite nanoparticles. The spikes indicate the reduction of individual hematite monomers at Au microelectrode. Inset: an enlarged view of a spike. (For interpretation of the references to color in this figure legend, the reader is referred to the web version of this article.)

for pH between 2.0 and 4.0 from the charge passed during the electro-reduction.

Assuming quantitative dissolution, the spherical diameter of the nanoparticles are determined by using the following equation: [20,22]

$$Q = \frac{n\pi\rho F}{6M} d^3 \quad (1)$$

where  $Q$  is the integrated charge under a spike;  $n$  is the number of electrons per  $\text{Fe}_2\text{O}_3$  unit ( $=2$ );  $\rho$  and  $M$  are the density ( $=5.3 \text{ g cm}^{-3}$ ) [23] and molar mass ( $=159.678 \text{ g mol}^{-1}$ ) of the iron oxide;  $F$  is the Faraday constant ( $=96,485.3 \text{ C mol}^{-1}$ ); and  $d$  is the particle diameter. The size distributions of hematite nanoparticle obtained using Eqn. 1 are summarized in Fig. 4a. It should be noted that the present detection technique tends to be skewed towards smaller sized particles. This is because the probability of particle-electrode collision is higher for particles with a greater diffusion coefficient, which is inversely related to the size (Fig. 5) [24]. This can be corrected by normalizing the size distribution based on the diffusion coefficients of spherical particles with different sizes [13]. This treatment has been applied to the histograms shown in Fig. 4a.

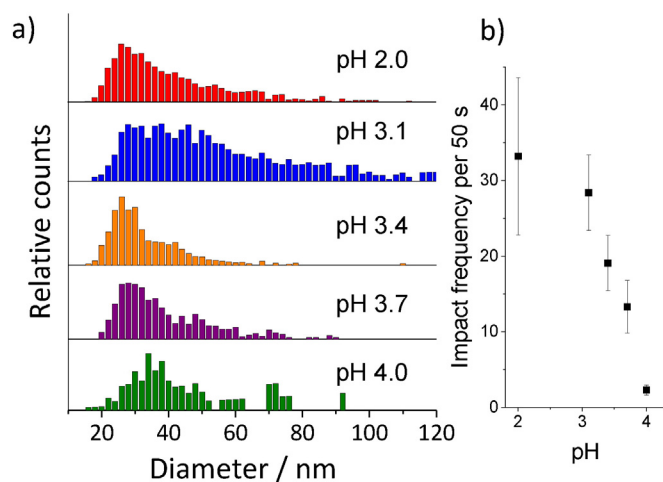


**Fig. 4.** a) Histograms of the particle size distribution based on the particle-impact chronoamperometric analysis at each pH. b) Impact frequency (number of spikes observed per 50 s) with respect to pH. Standard error of the mean is shown in the figure.

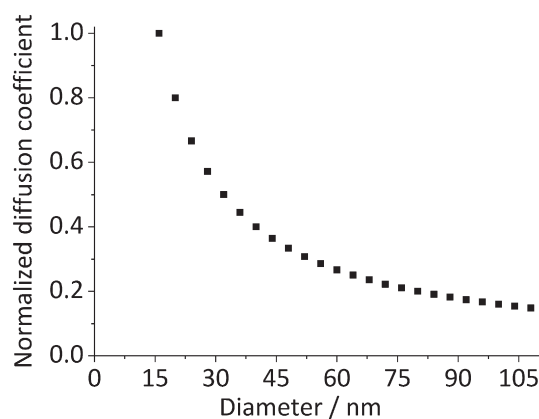


**Fig. 5.** Normalized diffusion coefficient of spherical nanoparticles with respect to the diameter. Diffusion coefficient is calculated using the Einstein-Stokes equation and normalized to that of the particle with 16 nm in diameter.

The histogram for pH 2.0 (Fig. 4a, top) shows the average diameter of  $31.8 \pm 3.7$  nm. This and the size distribution are in reasonable agreement with that of monomers observed from TEM images. The histograms of other pH show largely similar size distributions whereas the impact frequencies decrease with pH (Fig. 4b), which is in line with the advanced cluster formation shown by the NTA result. It is therefore suggested that the particle-impact method has not detected any large particles indicative of cluster formation in spite of the earlier analysis. This inconsistency may be interpreted as that there is no sufficient ionic strength or that clusters do not have fast enough diffusion to be detected by the electrochemical method. While these scenarios could be probable for exceedingly large clusters, this is not the case for small clusters (such as dimers and trimers). A previous report [10] has demonstrated that the ionic strength of 20 mM is sufficient for the range of particle size that is investigated in this study. Furthermore, diffusion coefficients for dimer and trimer can be estimated [25] and are reportedly comparable to that of monomers: the relative diffusion coefficient of a trimer to that of a monomer of the same hydrodynamic size is 0.62 [14]. This ratio is equivalent to the relative difference in the diffusion coefficients of one monomer with 32 nm in diameter and of the other with 52 nm. Since monomers of the latter size are clearly detectable by the particle-impact method, dimers and trimers must have also been observed. In other words, the diffusion coefficient of the suspended entities cannot be used to vindicate the lack of response from clusters during the particle-impact. Consequently, it can be concluded that the particle-impact method primarily detects monomers in the case of  $\text{Fe}_2\text{O}_3$  nanoparticles. This, in turn, implies that the agglomeration/disagglomeration process is reversible within the voltammetric timescale. Moreover, in order for monomers to dominate the electrochemical response (be the dominant flux carrier), the rate of dissociation of monomers from agglomerates must be sufficiently fast. Based on a kinetic model for the monomer-cluster equilibrium described by Sokolov et al. [14], monomers are formed via dissociation of clusters at the rate of  $20 \text{ s}^{-1}$  or faster.

Considering the above discussion, following analyses can be made for the histogram generated at different pH (Fig. 4a). At pH 3.1, the relative number of particles above about 45 nm in diameter is seemingly increased. This can be interpreted as that the number of the dominant particle sizes (i.e. below about 45 nm in diameter) has decreased due to the shift in the particle-cluster equilibrium towards agglomeration for the smaller particles. Such a size effect is explained by the DLVO theory as that the smaller particles are more prone to form clusters due to the lower electrostatic repulsion than the larger ones [15]. In addition, this can be confirmed by the histogram at pH 3.4, which shows a similar size distribution as pH 2.0 because the agglomeration equilibria of larger particles have also shifted away from monomers. The gradual shift of the mode of the size distribution to the larger diameters as pH increase

from 2.0 to 4.0 provides further evidence of the size effect on the *reversible* agglomeration/dis-agglomeration process, and the declining impact frequency with pH is indicative of a shift of the overall equilibria towards cluster formation.

In conclusion, the NTA and particle-impact chronoamperometry are successfully employed to show that fast *dynamic* equilibrium exists between hematite individual nanoparticles and agglomerates in 20 mM KCl. It is also found that the equilibrium shifts towards the cluster formation as pH increases as expected from the declining surface potential of hematite. Under the electrochemical approach, individual hematite nanoparticles dissociated from the clusters are detected as the Brownian motion results in a collision with a stationary electrode generating spikes in a chronoamperogram. The size of a nanoparticle is determined from the charge passed during the electro-reductive dissolution. This technique reveals that dynamics of hematite agglomeration is rapid and reversible and that the equilibria shift gradually towards cluster formation as pH increases. The successful application of the particle-impact chronoamperometry in this study opens a new way to investigate the colloidal behavior of mineral nanoparticles in aqueous solutions.

### Acknowledgement

This work was supported by a Marie Skłodowska-Curie Intra-European Fellowships (# 626320) (KS) and the European Research Council (FP/2007–2013/ERC Grant Agreement no. [320403]) (SVS) within the 7th European Community Framework Programme.

### References

- [1] R.M. Cornell, U. Schwertmann, *The Iron Oxides: Structure, Properties, Reactions, Occurrences and Uses*, Second Edition - Cornell - Wiley Online Library, second ed. Wiley-VCH, Weinheim, 2003.
- [2] G. Segev, H. Dotan, K.D. Malviya, A. Kay, M.T. Mayer, M. Grätzel, A. Rothschild, *Adv. Energy Mater.* 6 (2016) 1500817.
- [3] J. Hur, M.A. Schlautman, 264–270. *J. Colloid Interface Sci.* (2004) 277.
- [4] B.M. Smith, D.J. Pike, M.O. Kelly, J.A. Nason, *Environ. Sci. Technol.* 49 (2015) 12789–12797.
- [5] A.A. Keller, S. McFerran, A. Lazareva, S. Suh, *J. Nanopart. Res.* 15 (2013) 1692.
- [6] A.L. Dale, E.A. Casman, G.V. Lowry, J.R. Lead, E. Viparelli, M. Baalousha, *Environ. Sci. Technol.* 49 (2015) 2587–2593.
- [7] A.D. McNaught, A. Wilkinson, M. Nic, J. Jirat, B. Kosat, A. Jenkins (Eds.), *IUPAC Compendium of Chemical Terminology*, 'IUPAC Gold Book', second ed., vol. 79, Blackwell Scientific Publications, Oxford, 2007.
- [8] A. Maskara, D.M. Smith, *J. Am. Ceram. Soc.* 80 (2005) 1715–1722.
- [9] V. Filipe, A. Hawe, W. Jiskoot, *Pharm. Res.* 27 (2010) 796–810.
- [10] T.R. Bartlett, S.V. Sokolov, R.G. Compton, *ChemistryOpen* 4 (2015) 600–605.
- [11] N.V. Rees, *Electrochem. Commun.* 43 (2014) 83–86.
- [12] M. Pumera, *ACS Nano* 8 (2014) 7555–7558.
- [13] S.V. Sokolov, K. Tschulik, C. Batchelor-McAuley, K. Jurkschat, R.G. Compton, *Anal. Chem.* 87 (2015) 10033–10039.
- [14] S.V. Sokolov, E. Kätelhön, R.G. Compton, *J. Electroanal. Chem.* (2016), <http://dx.doi.org/10.1016/j.jelechem.2016.01.023>.
- [15] Y.T. He, J. Wan, T. Tokunaga, *J. Nanopart. Res.* 10 (2007) 321–332.
- [16] K. Shimizu, A. Shchukarev, J.-F. Boily, *J. Phys. Chem. C* 115 (2011) 6796–6801.
- [17] R.L. Blake, R.E. Hessevick, T. Zoltai, L.W. Finger, *Am. Mineral.* 51 (1966) 123–129.
- [18] S.V. Sokolov, E. Kätelhön, R.G. Compton, *J. Phys. Chem. C* 119 (2015) 25093–25099.
- [19] N. Kallay, Dojnović, A. Čop, *J. Colloid Interface Sci.* 286 (2005) 610–614.
- [20] K. Shimizu, K. Tschulik, R.G. Compton, *Chem. Sci.* 7 (2016) 1408–1414.
- [21] E. Kätelhön, E.E.L. Tanner, C. Batchelor-McAuley, R.G. Compton, *Electrochim. Acta* 199 (2016) 297–304.
- [22] K. Tschulik, B. Haddou, D. Omanović, N.V. Rees, R.G. Compton, *Nano Res.* 6 (2013) 836–841.
- [23] J.W. Anthony, R.A. Bideaux, K.W. Bladh, M.C. Nichols, *Handbook of Mineralogy, Mineral Data Publishing*, Tucson, Arizona, 1997 239.
- [24] J. Ellison, K. Tschulik, E.J.E. Stuart, K. Jurkschat, D. Omanovic, M. Uhlemann, A. Crossley, R.G. Compton, *ChemistryOpen* 2 (2013) 69–75.
- [25] M. Hoffmann, C.S. Wagner, L. Harnau, A. Wittemann, *ACS Nano* 3 (2009) 3326–3334.